Mechanics of Advanced Composite Structures

Journal homepage: https://macs.semnan.ac.ir/

Semnan University

ISSN: 2423-7043

Research Article

Analyzing and Improving Flexural and Impact Strength of Composites Enhanced with Nanoparticles and Natural Fibers

Hossein Taghipoor [a*], Jaber Mirzaei [b]

[a] *Faculty of Mechanical Engineering, Velayat University, P.O. Box 99111-31311, Iranshahr, Iran*

[b] *Faculty of Mechanical Engineering, Semnan University, Semnan, Iran*

ARTICLE INFO

Article history:

Received: 2023-12-08
Revised: 2024-03-19
Accepted: 2024-03-25

Keywords:

Multi-Objective optimization;
Mechanical properties;
Modeling;
Response surface method (RSM);
Bio-composite.

ABSTRACT

One of the enormous challenges of bio-composites is the improvement of the flexural and impact strength. Therefore, the optimization and parametric investigation of nanocomposites reinforced with natural hybrid fibers is the main focus of this study. Kenaf/basalt/nanographene fibers in polypropylene were used to reinforce bio-composite specimens. Response Surface Method (RSM) was applied to study and present a mathematical model for the performance of bio-composite according to a number of parameters including the basalt fiber weight percentage, kenaf fiber as well as nanographene. The performance of the specimens was discussed under the bending and impact tests and the outcomes were explained by the use of FESEM images. The optimal value of the parameters was set as a multi-objective according to the increase of the flexural strength and energy absorption, the reduction of the specimens' weight, and also a Pareto diagram was illustrated considering the design goals. The findings revealed that the composite specimen with the best flexural behavior had the flexural strength of 51.2558 MPa, which consisted of 0.8723 wt% of basalt fibers, 15% of kenaf fibers, and 0.76881% of graphene nanoparticles. In addition, the best specimen in terms of impact had 116,809 J / m energy absorption, which included 8.23% basalt fibers, 0.808% graphene nanoparticles, and 15% kenaf fibers.

1. Introduction

To research new polymeric materials and acquire their technology, natural fibers are extensively available worldwide [1]. Various polymers with petroleum-based origins are widely applied in natural fibers, for example, bamboo, jute, hemp, banana, kenaf, sisal, etc. [2]. Currently, due to the increasing use of reinforced and stable composites, their application in the civil engineering, automotive industry, and manufacturing industries is rapidly expanding [3]–[5]. Kenaf is one of the important natural fibers used as support for polymer-matrix composites. Kenaf fiber is considered an important source for composite materials and other industrial applications [6]. It serves as an important source of cellulose with benefits in economic as well as environmental fields. In three months (after seeds are sowed), it can grow in extensive areas of climates, and its height reaches 3 meters with a diameter of 3-5 cm [7]. Kenaf filaments contain individual fibers that are typically 2-6 mm. Its structure is similar to synthetic fiber-reinforced composites. Scientists believe that the general characteristics of kenaf fiber depend upon the intrinsic attributes of its individual components [8]. The stiffness and

* **Corresponding author.**
E-mail address: h.taghipoor@velayat.ac.ir

Cite this article as:
Taghipoor, H., and Mirzaei, J., 2024. Analyzing and Improving Flexural and Impact Strength of Composites Enhanced with Nanoparticles and Natural Fibers. *Mechanics of Advanced Composite Structures*, 11(2), pp. 467-482
https://doi.org/10.22075/MACS.2024.32607.1593

strength of fibers using cellulose components are due to hydrogen bonds and other bonds. In ancient times, people competently used kenaf as a rope, fabric, and sack. Recently, in order to prevent deforestation, it was applied as a substitute for raw materials instead of the wood used in the paper industry. In addition, kenaf fibers are used in manufacturing non-metallic materials in the automotive and textile industries [9]–[11]. Due to increased levels of aspect ratio and hardness in composites in comparison with other fibers, kenaf stem fibers make an important contribution to strengthening thermoplastic composites. The kenaf fiber module and tensile strength are 60 and 11.9 GPa, respectively [12].

In a study, Jay et al. [13], explored the impression of the jute fibers' weight percentage on the thermal and mechanical characteristics of composites. They applied fibers at 25 to 50 wt%. The results of their study show that by increasing fibers up to 30 wt%, the flexural and tensile performance of the composite will be enhanced. They also claimed that by boosting the weight percentages of fibers at higher levels, the mechanical attributes will be decreased. Yu et al. [14], explored the mechanical properties of natural short fiber-reinforced composites. They applied rum and jute fibers the length of 10 mm (average length) and 10 to 50%wt. It appeared that the highest growth in mechanical performance happened at 30 wt% of the fibers. Loperesto et al. [15], examined the mechanical performance of the composites supported by basalt fibers and glass. The specimens' preparation was done using vacuum bagging technology and also a tensile test was performed using an MTS machine. It was found that the composite reinforced with basalt fibers includes higher young modulus, flexural and compressive strength, and higher energy absorption as well as impact resistance. Along similar lines, Wu et al. [16] studied the epoxy composites and basalt fibers' tensile performance in a corroding environment. Wu et al. [17], also explored the fatigue behaviors of various FRP compounds constructed by basalt fiber, glass, carbon, and hybrid fibers. They found that carbon/basalt hybrid composites considerably enhanced fatigue endurance capacity. Banibayat and Patnaik [18], researched the mechanical behavior of basalt fiber-supported polymer tape, which has been produced by the use of the wet layup approach. In an attempt to improve the mechanical behavior of concrete, Hai et al. [19], applied basalt fibers as the flexural reinforcement for concrete components as well as short basalt fibers.

All over life, fiber-reinforced structures may be exposed to dynamic loads, e.g. explosion and impact. The CFRP/GFRP was also found effective in reinforcing structures against explosive loads and impact [20]. However, few studies have been done on how BFRP products can reinforce structures against explosions and impact resistance.

Furtos et al. [21], explored the reinforcing impression of woven and unidirectional glass fibers upon the flexural strength and flexural modulus in glass fiber-reinforced composites. They found that increasing the degrees of glass fiber in the composites results in flexural strength and modulus improvement. In another work, they used alkaline-resistant glass fibers and obtained new biomedical glass fiber resin cement with enhanced mechanical attributes and radiopacity. The mechanical attributes increase in the order light-curing < self-curing < dual-curing [22]. Ralph et al. [23] explored the amount of energy absorption tensile strength and tensile modulus of polymer composite supported by short basalt fibers. They concluded that by adding the volume percentage of basalt fibers, tensile modulus improved to 110% and tensile strength to 64%, but with increasing the basalt fibers volume percentage, the impact strength decreased.

Due to its distinctive characteristics, nano-graphene has been known as a favorite material in nanotechnology in recent years [24]. Moreover, graphene is naturally available, so its use is usually economical owing to its unique properties. Having a rather low cost, and good thermal and mechanical attributes, this material along with the use of graphene nanoparticles, has made a new possibility for the growth of polymer nanocomposites [25].

Song et al. [26], reported that the 1 wt% inclusion of graphene nanosheets to polypropylene enhanced its tensile strength and yield strength. According to their report, the addition of more than 1 wt% (up to 5 wt %), diminished the compound's strength. In another study, Yuan et al. [27], investigated the mechanical attributes of polypropylene/graphene oxide nanocomposites. Their findings demonstrated that up to 1 wt% of graphene oxide presence while increasing the tensile strength and elastic modulus will diminish extension at the break.

In this research, basalt and kenaf fibers are blended with nanographene in order to enhance the cohesion with Polypropylene. Then we have the addition of the nanoparticles to the polymer matrix to obtain improved mechanical behavior. The purposes of this research are to explore the coincident impact of the basalt and kenaf fiber loading and nanoparticle content on the impact and flexural strength of bio-composites in natural fiber, and independent variables are optimized in order for the flexural and impact strength of the

bio-composite to be maximized. Moreover, the morphology exploration of the bio-composites is done as well.

2. Experimental Details

2.1. Materials

Polypropylene polymer produced by Arak Petrochemical Company under the trade name V30S was applied to make composite specimens. Besides, the most common natural reinforcement for polymer-based composites is kenaf fibers which have a density of $75 \times 10^3 \frac{Kg}{m^3}$ and a diameter of 50 microns and are created entirely of natural materials. Based on the datasheets presented by the manufacturer, these fibers possess a tensile strength of 240-930 MPa, a Young GPa modulus of 14-53, and elongation at break of 1.6-2.9%. Basalt fibers produced by Basaltex Company with a 20 microns diameter and a $\frac{0}{75} \times 10^3 \frac{Kg}{m^3}$ density have been used in this research. Based on the manufacturer's reported datasheet, these fibers have 4930-1430 MPa tensile strength, 110-71 GPa Young modulus, and 3.3-1.3% elongation at break [28].

Graphene powder produced by X-G Science USA and with the trade code xGnP-C750 was employed as a nanofiller in this research. Based on the product's technical data sheet, these black powders are specific kinds of nanoparticles that contain a small number of graphene sheets within the structure of small plates. Having an average diameter of fewer than 5 microns, a surface area of 750 m2/g, a thickness of 2 nm, and a density of $\frac{2}{2} \times 10^3 \frac{Kg}{m^3}$, these powder particles were identified. Based on the reports of the manufacturer, these graphene nanosheets can improve the mechanical characteristics, such as stiffness, hardness, and strength of the substrate surface, and are compatible with almost all polymers. According to the information provided, to make these nanosheets, non-oxidizing processes have been used. Therefore, these materials have a graphite surface of carbon molecules with a 2SP structure, which makes them suitable for applications requiring electrical and thermal conductivity.

2.2. Preparation of the Fiber-reinforced Nanocomposites

Every specimen in this research was prepared by melt compounding perspective by the use of an internal mixer model HBI SYS 90, which is a product of Hack Company of America by the speed of 60 RPM at 180°C. Following the melting of polypropylene in an internal mixer, basalt fibers, graphene, and kenaf fibers were mixed in the special weight percentages and with similar conditions, with 10 min of mixing time for every single specimen. After determining the weight percentage of each composite, they were weighed and their physical composition was done. Based on the internal mixer chosen for mixing and baking materials and the 60 cubic centimeters capacity of the material chamber of this machine, the values of their components were weighed according to their weight percentages. Standard specimens of mechanical properties tests were obtained by the use of compression molding with a heat press machine, manufactured by the Japanese Toyoski VCH model, at 2.5 MPa and 200 °C. This press machine was employed in three steps. First, the material was preheated for 10 minutes. Subsequently, the heating element was switched on and the pressure and the temperature were set at 2.5 MPa and 200 °C, respectively. After 20 minutes, the element was switched off, and in order to prevent the burning and thermal degradation of the material, a water cooler was employed. Eventually, the specimens arrived at room temperature and were then removed from the molds.

2.3. Bending

For the measurement of the specimens' flexural strength, the bending test (three-point bending) was done using the Santam device with a capacity of 15 tons under the ASMT D790 standard, [29]. This experiment was conducted on rectangular cubic specimens with dimensions of 125 × 12 × 5 mm at a loading speed of 1.3 mm/min and a length of 50 mm. Therefore, the specimens' flexural strength was measured by the Eq. 1.

$$the\ \sigma_f = \frac{3fl}{2bh^2} \quad (1)$$

where b is the specimen width, h is the specimen thickness, l is the effective length tested, and f represents the force exerted by the testing machine.

2.4. Impact

An impact test (Izod) was run to assess the specimens' strength and also their fracture resistance. For impact properties, the rectangular cube specimens with notches in the middle were constructed following the ASTM D256 standard, [30].

Fig. 1 indicates the specimen made according to this regulation. The Izod test was run at the temperature of the room using the 958 CEAST Tester. The amount of absorption energy into the fracture specimens can be calculated by Eq. 2.

$$E=Mg(h_1 - h_2) \quad (2)$$

in this equation, E is the energy absorbed, g is the gravity acceleration, M is the specimen mass, and h1 and h2 show the first and second height of the impactor, respectively. After the prepared

specimens underwent the mechanical impact test, the analysis of the results was done and they were compared by the use of the Response Surface Method.

Fig. 1. Standard specimen of the impact test

3. Experimental Data

In order to evaluate the impression of each introduced nanocomposite component and determine the relationship between each component, namely basalt fibers, graphene nanosheets, as well as kenaf fibers in the matrix of polypropylene polymer, Statistical methods were used. Because there are restrictions in the highest possible extent of fibers applied in the polymer matrix, the number of graphene nanosheets in the weight percentage range from 0 to 1.5%, kenaf fibers and basalt fibers in the range from 0 to 15% were added to the polypropylene matrix to quantify the number of selected materials in terms of weight percentage in this study.

Moreover, for each of these tests, three standard specimens were chosen from each specimen. After identifying the range of materials applied to create nanocomposites derived from the response surface test design and Box-Behnken approach, the mixing approach and the number of compounds is indicated and presented in Table 1. Table 2 points out the average test outcomes for two responses to the flexural and impact strengths after impact and bending tests.

Table 1. Different amounts of ingredients at weight

code	polypropylene (%wt)	graphene (wt%)	kenaf fibers (%wt)	basalt fibers (%wt)
1	99.25	0.75	0	0
2	84.25	0.75	0	15
3	84.25	0.75	15	0
4	69.25	0.75	15	15
5	92.50	0	7.5	0
6	77.50	0	7.5	15
7	91.00	1.5	7.5	0
8	76.00	1.5	7.5	15
9	92.50	0	0	7.5
10	77.50	0	15	7.5
11	91.00	1.5	0	7.5
12	76.00	1.5	15	7.5
13	84.25	0.75	7.5	7.5
14	84.25	0.75	7.5	7.5
15	84.25	0.75	7.5	7.5

Table 2. The outcomes of various tests as well as error values

Specimen code	Flexural strength (MPa)	Weight of bending test specimens (g)	Impact strength (J/m)	Weight of impact test specimens (g)
1	43±0.59	2.2±0.004	85.69±0	1.169±0.001
2	48±0.76	2.90±0.065	105.17±1	1.6±0.002
3	50±0.6	2.14±0.044	102.34±1	1.38±0.002
4	55±0.85	2.7±0.0329	128.97±0	1.4±0.001
5	42±0.98	2.14±0.0578	76.49±0	1.14±0.002
6	47±0.8	2.90±0.049	94.07±1	1.6±0.002
7	45±0.19	2.20±0.01	78.86±0	1.16±0.002
8	50±0.33	2.90±0.086	107.57±0	1.6±00.001
9	39±0.01	2.45±0.0283	70.34±1	1.2±0.003
10	49±0.01	2.20±0.027	93.63±0	1.18±0.0015
11	44±0.5	2.55±0.014	79.82±0	1.3±0.001
12	50±0.6	2.45±0.036	106.42±1	1.2±0.001
13	49±0.01	2.45±0.001	104.75±0	1.2±0.001
14	49±0.8	2.49±0.0624	103.83±0	1.19±0.0015
15	50±0.6	2.66±0.036	102.55±0	1.18±0.001

4. Results and Discussion

In this research, DOE (a statistical test) was fulfilled to identify the Impact and Flexural Strength in the case of composites. The influence of the design variables on the responses is assessed using the Design-Expert software. The purpose of the design of experiments (DOE) approach is to supply estimated response surfaces that are adequately correct to take the place of the true response and can be employed to achieve the optimal points of parameters.

4.1. Bending Strength

The outcomes of the regression test of the flexural strength response provided a second-order model. The values obtained for R2 and R-adj2 were 0.9866 and 0.9792, respectively, indicating the capability of the output model to forecast the response performance. Moreover, the power response of the flexural strength was considered as the exponent 2 to increase the correctness of the output model and improve the normality. The last equation is as follows.

Now that the values associated with column P for the independent factors, squares (graphene × graphene), and the interaction effects between the factors (hemp × graphene) are less than 0.05, this means that the impact of these factors on the flexural strength with 95% confidence is great. Thus, the equation of regression for the flexural strength is in the form of equation (3):

$$\begin{aligned}&(\text{Flexural strength})^2\\&= +1335.19370 + 32.74741 \times \text{Basalt fiber}\\&+57.69745 \times \text{Kenaf fiber}\\&+1181.6351 \times \text{Geraphen}\\&-13.32844 \times \text{Kenaf fiber} \times \text{Geraphen}\\&-603.14406 \times \text{Geraphen}^2\end{aligned} \quad (3)$$

Figure 2(a) shows the sensitivity of the flexural strength to the change of the percentage parameters of graphene nanoparticles, basalt, and kenaf fibers. As shown, adding kenaf fibers and basalt fibers to the matrix of the polymer has increased the bending strength. Between these two fibers, due to the higher slope of the kenaf fiber, sensitivity to the changes of these fibers is more in the flexural strength. The impact of the basalt and kenaf fibers on the waste of energy in crack boosting in the bending test specimens results in increasing the flexural strength [31], [32]. In addition, adding graphene to the presented composition has boosted flexural strength. It is observable in the graphs that the existence of only 0.75 wt% of the graphene nanosheets in the composition of the specimens enhanced the flexural strength, which is caused by the improvement of the bond between the substrate and the fibers. Moreover, the presence of nanosheets by several mechanisms including making holes, bridging, and deviating from the crack path can be an obstacle to crack growth and increase the energy of fracture by absorption of higher energy.

However, in the specimens having 1.5 wt% of graphene nanosheets, the flexural strength has diminished in comparison to 0.75 wt% of graphene. That is, in the specimens with more content nanoparticles, the formation of lumps is observed that may yield stress concentration and create areas for the initiation of the crack growth and finally result in a more brittle material [26], [33].

Figures 2-(b) to 4-(d) show the response approaches according to flexural strength. As presented in process (b), the consistency of the graphene weight percentage and the increase in the basalt fibers and the kenaf fibers weight percentage increased the flexural strength.

Also, it can be concluded from process (c) that the consistency of the kenaf fibers' weight percentage as well as the increase in the basalt fibers' weight percentage lead to great flexural strength, and by adding graphene up to 0.75 wt% of graphene enhances the bending strength, and adding with greater weight percentages weakens the bending strength. Also, it is concluded from process (c) that by kenaf fibers' weight percentage being still constant, boosting the basalt fibers weight percentage also boosts the bending strength, and increasing graphene up to 0.75% weight of graphene boosts it and adding it in higher weight percentages decreases the flexural strength [34].

As observable in process (d), the consistency of the basalt fibers weight percentage as well as the improvement in the kenaf fibers weight percentage increases the flexural strength. Moreover, adding the graphene weight percentage improved the flexural strength at first and then decreased it [35].

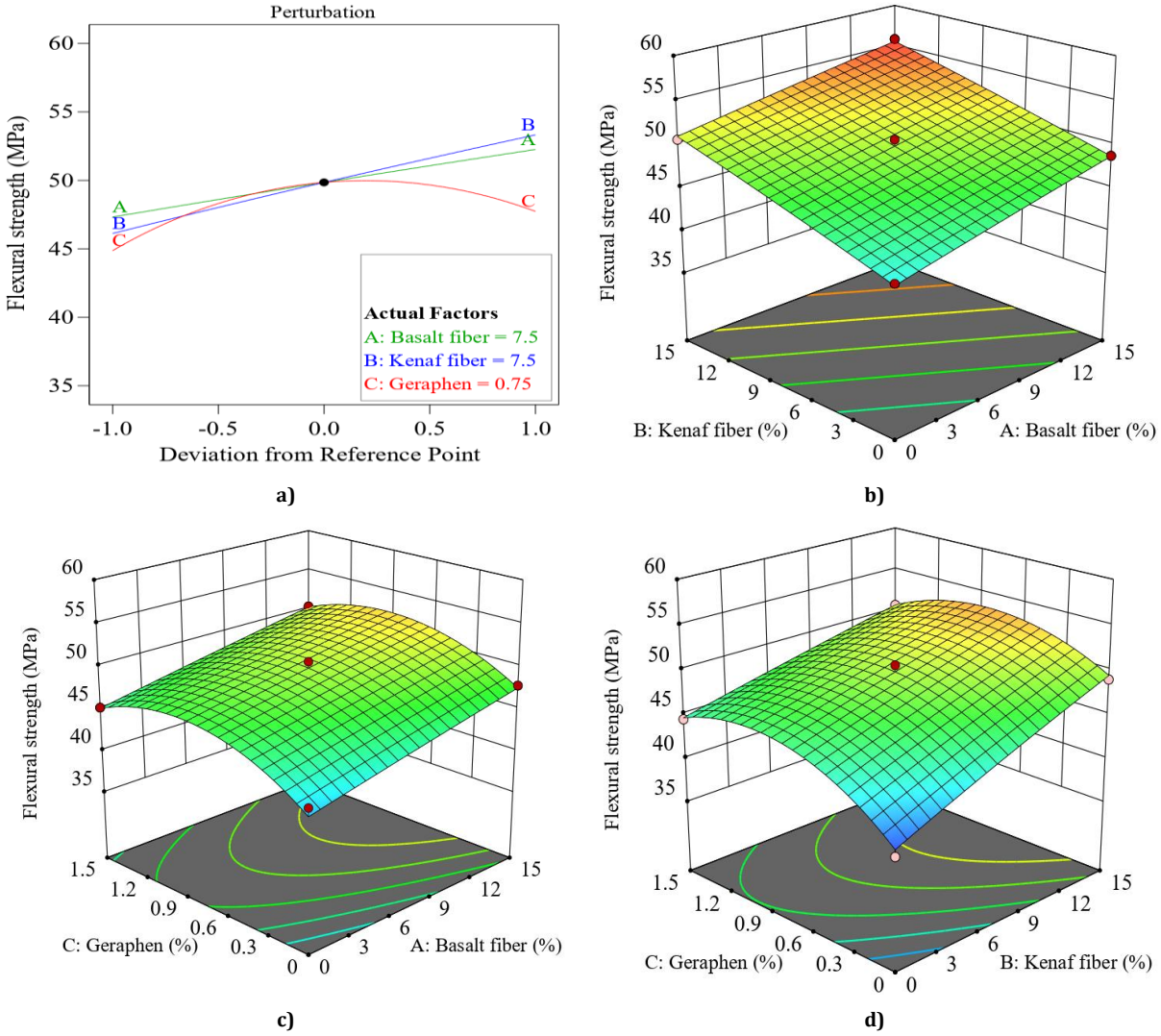

Fig. 2. Diagrams of a) saturation b to d response distribution for flexural strength response at; b) basalt fibers and kenaf fibers; c) basalt fibers and nanographene; d) kenaf fibers and nanographene

4.2. Impact Energy Response

The outcomes of the regression test of the impact strength response present a non-linear model amidst the percentage parameters of basalt, kenaf fibers, and graphene nanoparticles. The values for R^2 and R-adj^2 were 0.9859 and 0.9781, respectively, indicating the capability of the output model to make predictions on response performance. Considering the P-value of less than 0.05 for the importance of the effect of the parameters of the percentage of basalt, kenaf fibers, and graphene nanoparticles, the second-order term for the parameter of the kenaf fibers and basalt percentage and the binary interaction between nano-graphene and kenaf fibers as well as the binary relationship amidst basalt and kenaf fibers have been omitted. Equation (4) is the final regression equation for the impact strength:

$$\begin{aligned} &Impact\ strength \\ &= 63.125 + 1.1833 \times Basalt\ fiber \\ &+1.5 \times Kenaf\ fiber \\ &+45.88 \times Geraphen \\ &+0.488 \times Basalt\ fiber\ \times\ Geraphen \\ &-28.92 \times Geraphen^2 \end{aligned} \quad (4)$$

As illustrated in Fig. 3-(a), adding fibers of kenaf and basalt to the matrix of polymer increased the impact strength. The impression of the basalt and kenaf fibers on the waste of energy in crack boosting in the grooved specimens in the test of Charpy increases the impact strength. Moreover, increasing the amount of graphene in the composition boosts the impact strength at first, but then, with the increase in the amount of nanographene, the strength of the specimens

under impact loading decreases. As can be observed in the graph of Fig. 3-(a), the presence of only 0.75 wt% of the graphene nanosheets in the composition of the specimens has led to an increase in the impact strength, which is because of the improvement of the bond between the substrate and the fibers. Also, the presence of nanosheets by various mechanisms namely bridging, making holes, and deviating from the crack path might be an obstacle to crack growth. In addition, absorbing higher energy increases the energy of fracture. However, the impact strength in the specimens with 1.5 wt% of the graphene nanosheets has decreased in comparison to 0.75 wt% of the graphene. In other words, in specimens with a great number of nanoparticles, we see the formation of lumps that might result in stress concentration and create conditions for the initiation of crack boosting and finally lead to a more brittle material [27], [33]. Figures 3-(b) to 3-(d) show the response processes which are related to the impact strength. As shown in process (b), by keeping the graphene weight percentage unchanged, the basalt fibers weight percentage increases and the kenaf fibers weight percentage also increases in a completely linear manner which has improved the impact strength [36].

It is also concluded from process (c) that with the kenaf fibers weight percentage being consistent, increasing the weight percentage of the basalt fibers and increasing the amount of graphene up to 0.75 wt%, the impact strength has increased, but adding graphene in greater weight percentages has decreased the impact strength [37].

As can be seen in process (d), with the basalt fibers' weight percentage being unchanged, the kenaf fibers' weight percentage increases, and the impact strength increases as well. Also, adding the graphene weight percentage improved the impact strength at first and then decreased it.

4.3. Morphological Studies of Graphene/PP /kenaf Fiber/ Nanocomposites and Basalt Fiber Composite

In order to scrutinize the structural behavior and morphological surface of the fracture of the tensile specimens, a Field Emission Scanning Electron Microscope (FESEM) with X-ray energy dispersive spectroscopy (EDS) in materials and energy research center (MERC), (Tehran, Iran) was used. To improve electrical conductivity and avoid electron gathering, the specimens' surface was covered with a narrow layer of gold using a machine for gold plating. The morphology of the surface serves as the key parameter for evaluating the structural behavior of the nanocomposites and determining how fibers and nanoparticles are related to the matrix.

Fig. 4 demonstrates the sample's fracture surface obtained from the pure polypropylene polymer specimen under the impact loading. As can be seen, the fracture surface indicates a brittle fracture, which forms a leaf-like shape on the surface of the fracture.

Fig. 5 demonstrates the fracture surface of the specimens which contains 7.5 wt% of the basalt fibers, 0.75 wt% of the graphene nanosheets, and 7.5 wt% of the kenaf fibers (specimens' number 13) under the impact loading. In addition, it shows the good distribution of the nanoparticles in the substrate and the lack of accumulation of nanoparticles in the matrix. Such a distribution has led to further clinging of the kenaf and basalt fibers to the matrix of the polymer. From Fig. 5, the fracture of basalt and kenaf fibers plays an important part in increasing the impact strength. Moreover, pulling out the basalt and kenaf fibers from the polypropylene under impact loading, which is accompanied by the substrate fracture, is considered another mechanism for absorbing the impact energy.

In Fig. 6, the adhesion level between the graphene nanosheets and the kenaf and basalt fibers can be easily seen. Other researchers also have reported the presence of graphene nanosheets in polymer nanocomposites [38].

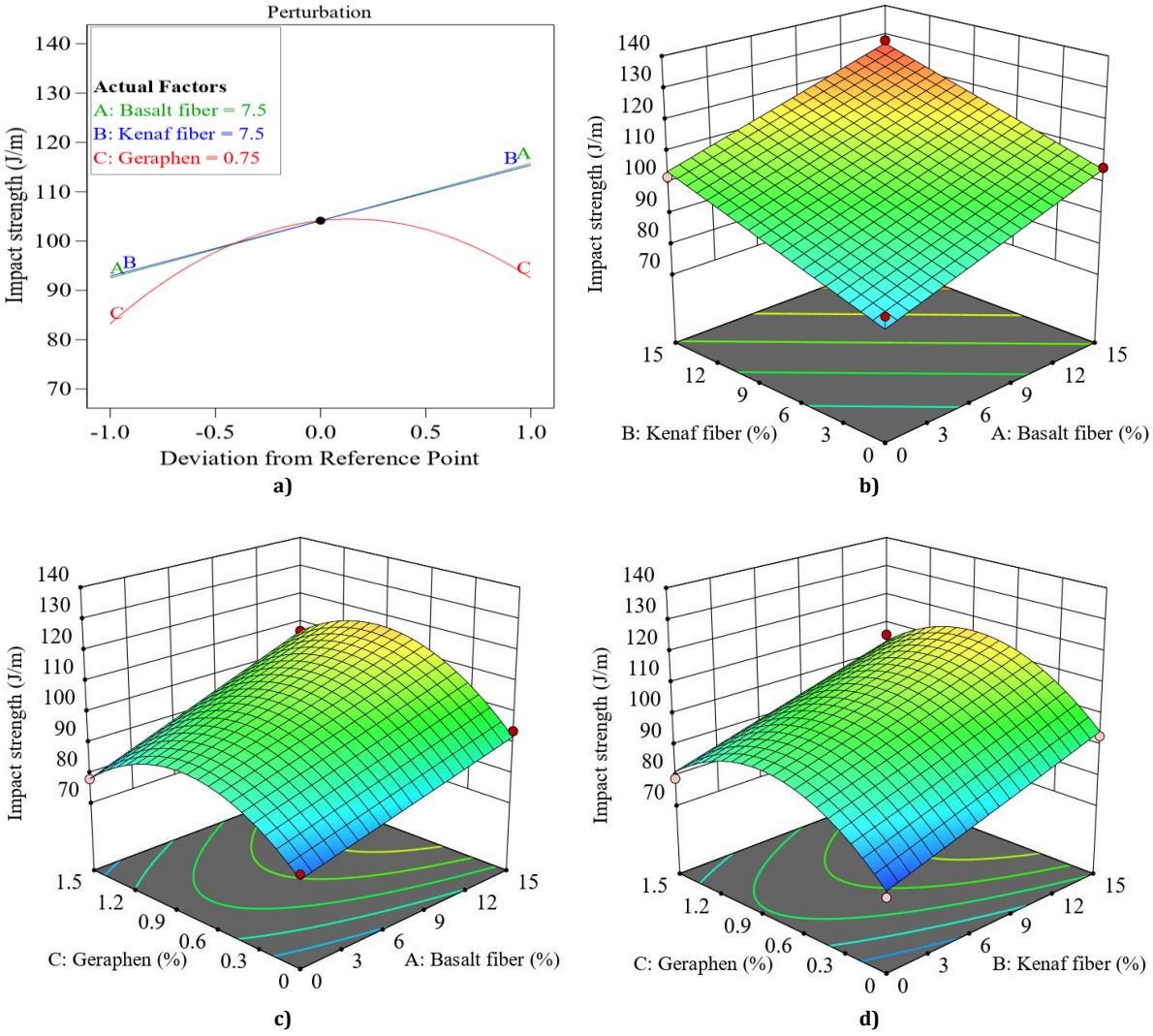

Fig. 3. Diagrams of a) saturation b to d response distribution for impact strength response at; b) basalt fibers and kenaf fibers; c) nanographene and basalt fibers; d) kenaf fibers and nanographene

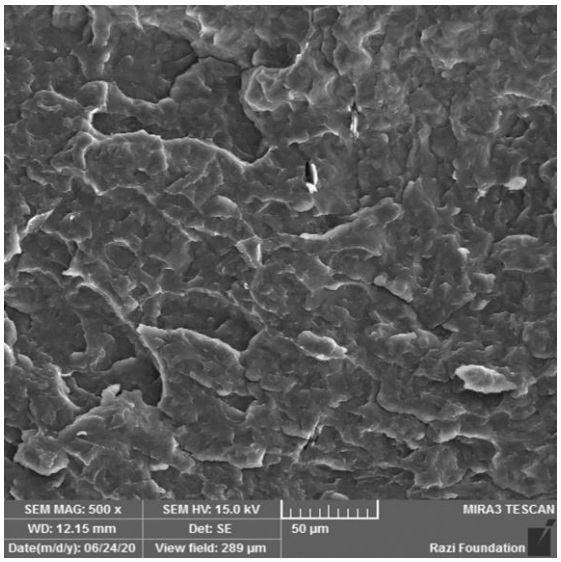

Fig. 4. Image of pure polypropylene specimens

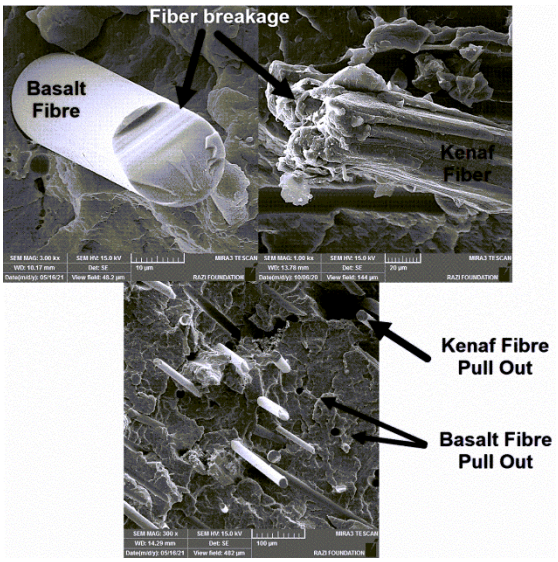

Fig. 5. Image of the fracture mechanism in specimen no. 13, under impact loading

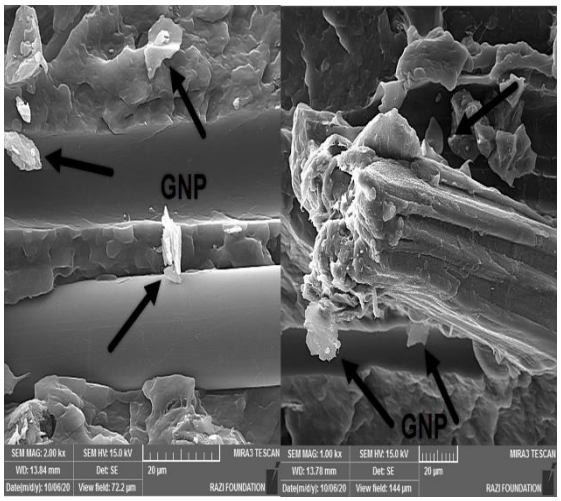

Fig. 6. Image of the nanographene in sample no. 13, under impact loading

Figure 7 illustrates the fracture surface of the specimen under the flexural loading containing 0.75 wt% of nanographene, 15% wt of basalt fibers, and 0 wt% of kenaf fibers. As shown in the figure, the fracture surface of the basalt fibers can be easily seen, which have been broken under the flexural loading [32]. Under flexural loading, the contribution of fiber fracture to increasing the strength and the pulling out of the fibers from the substrate is less recognized. However, despite the presence of 0.75 wt% of the nanographene, this protrusion is rarely seen especially in the basalt fibers, which showed the highest protrusion of the polypropylene under the impact loading.

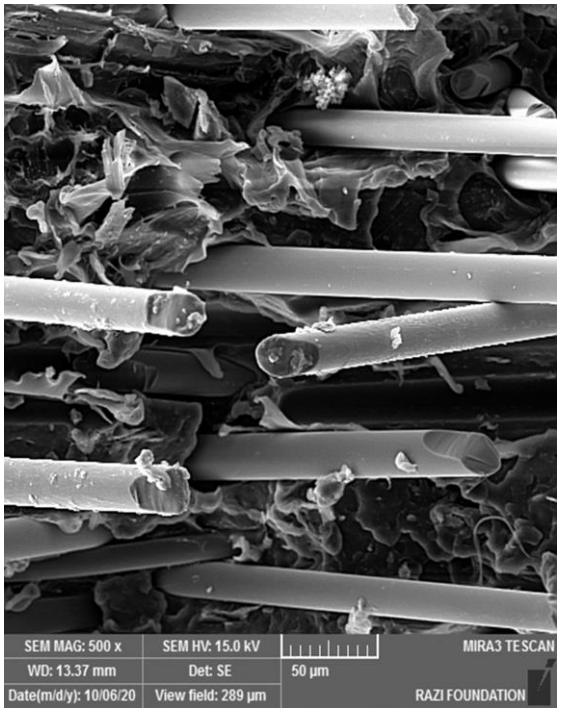

Fig. 7. FE-SEM picture which is captured on specimen no. 2, under the flexural loading

5. Optimization

Increasing the flexural and impact strength as a result of the experimental analysis, and simultaneously reducing the composite weight are the significant elements for design in this study. Hence, the components that are considered for the multi-objective optimization consist of gaining the highest value of the flexural and the impact strength and simultaneously the lowest weight value. The algorithm multi-objective particle swarm optimization was used for optimization in this article. Taken together, the multi-objective optimization method and parameters taken into account are equations 5 and 6:

$$\begin{cases} \text{Minimize } [-Impact, Weight] \\ s.t. \\ 0\% \le Kenaf\ fiber \le 15\ \% \\ 0\% \le Basalt\ fiber \le 15\ \% \\ 0\% \le Graphene \le 1.5\ \% \end{cases} \quad (5)$$

$$\begin{cases} \text{Minimize } [-Flexural\ strength\ , Weight] \\ s.t. \\ 0\% \le Kenaf\ fiber \le 15\ \% \\ 0\% \le Basalt\ fiber \le 15\ \% \\ 0\% \le Graphene \le 1.5\ \% \end{cases} \quad (6)$$

5.1. Multi-objective Optimization by Means of the Utility Function

Due to its convenience of use, easy access to Design-Expert software, adaptability of the weight percentage, and its potential to identify the significance of merits for each unique response, the Utility function method was used in this research. The multi-objective optimization problems can be solved with Design-Expert which uses the Utility method with an approach for blending the responses to a quantity without dimensions named the utility function. Specifically, the utility method involves moving each evaluated response to a unitless range as $0 < di < 1$, and therefore once di shows a greater value, the response has more efficacy. Table 3 indicates the scope of parameters, their wt %, and their impression according to the optimization used for each flexural and impact strength response.

Table 3. Values of the parameters with an effect on optimization

Upper limit	Lower limit	Goal	Unit	Parameters	Objective Functions
15	0		wt%	Basalt fiber	Flexural Strength and Weight
15	0		wt%	Kenaf fiber	
1.5	0		wt%	Geraphen	
55.85	39	Maximize	MPa	Flexural strength	
2.9	2.14	Minimize	g	Weight	
15	0		wt%	Basalt fiber	Impact and Weight
15	0		wt%	Kenaf fiber	
1.5	0		wt%	Graphene	
128	70	Maximize	MPa	Impact	
1.6	1.145	Minimize	g	Weight	

5.2. Multi-objective Particle Swarm Optimization (PSO)

Apart from the optimization using the utility function, the multi-objective particle swarm optimization was employed in this research to attain an optimal state of the impact and bending strength employing the output equations of the experiments' design outcomes. The PSO is a technique that draws on population and the main motivation behind its introduction was the collective movement of birds or fishes. This method was first introduced by Eberhard et al. [39]. Since the PSO method is convenient to implement and yields efficient results when computing it produced a greater achievement in comparison to other random optimization approaches. Because of its rapid coincidence and Pareto being well-distributed than other algorithms of multi-objective optimization, including PEAS, NSGA, etc, the PSO has been the issue of current interest.

5.3. Optimization Results

Considering the optimization done by the use of Design-Expert software based on table 3 and the algorithm of PSO as well as the requirements determined in equations 5 and 6, Pareto diagrams indicated the multi-objective optimization for the impact and flexural strength. The optimum points' graphs for the flexural and impact strength are displayed in Fig. 8. The total points shown in Fig. 8 for both optimization procedures include the best optimum points using the requirements of equations 5 and 6. Every single point is regarded as an optimum point.

Moreover, Figure 9 shows the kenaf fiber parameters, basalt fibers, and nanographene distributions as well as the alterations in the flexural strength responses, and Fig. 10 shows the kenaf fiber parameters, basalt fibers, and nanographene distributions, along with the alterations in impact strength responses.

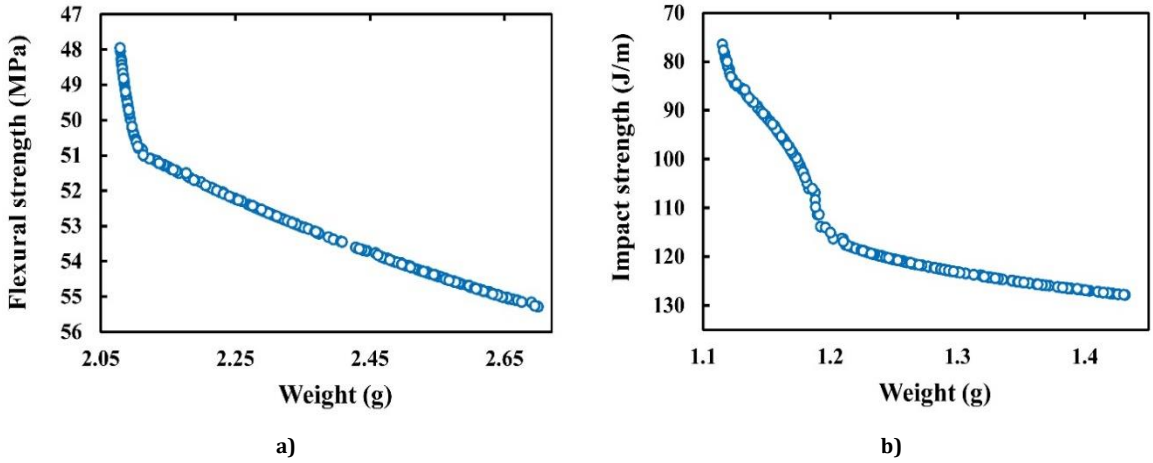

Fig. 8. Graph of the optimum points obtained using PSO for; (a) Flexural, and (b) Impact strength

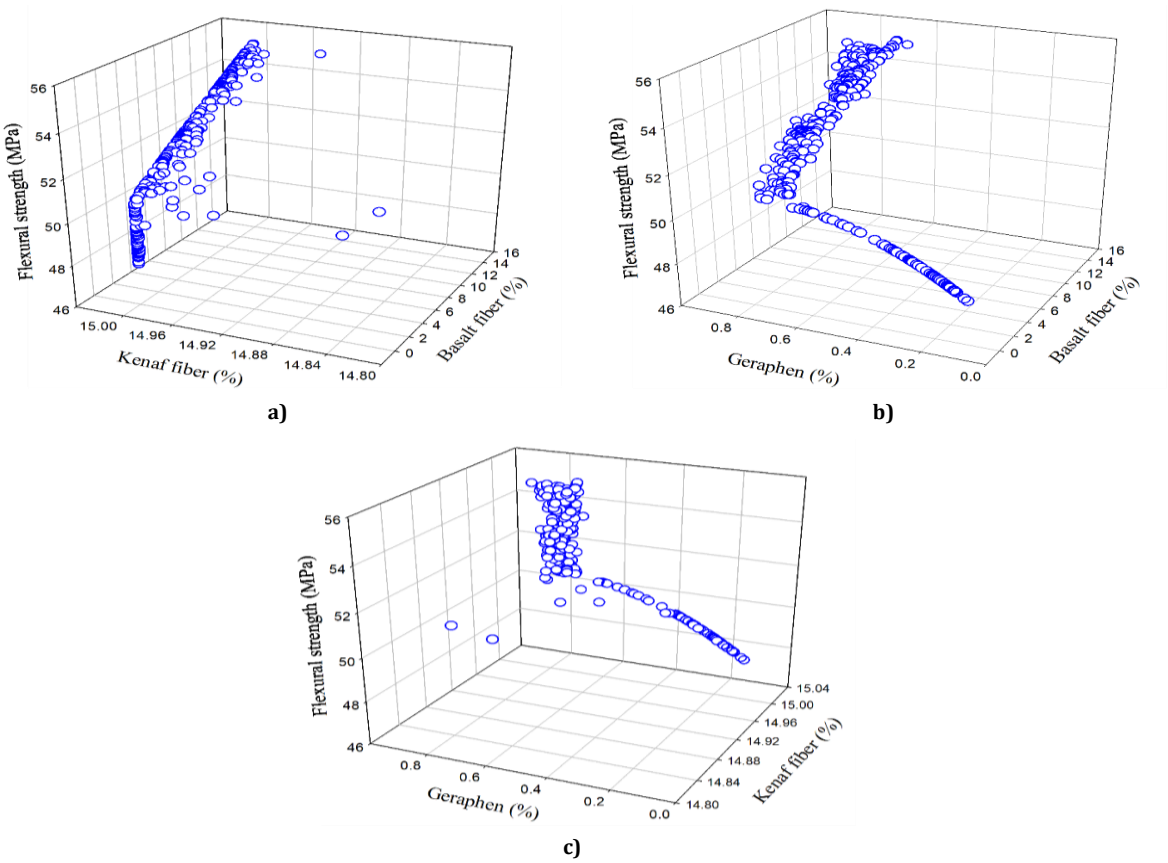

Fig. 9. Design variables distribution a) basalt fibers and kenaf fibers; b) basalt fibers and nanographene; c) kenaf fibers and nanographene in the best condition to boost the flexural strength

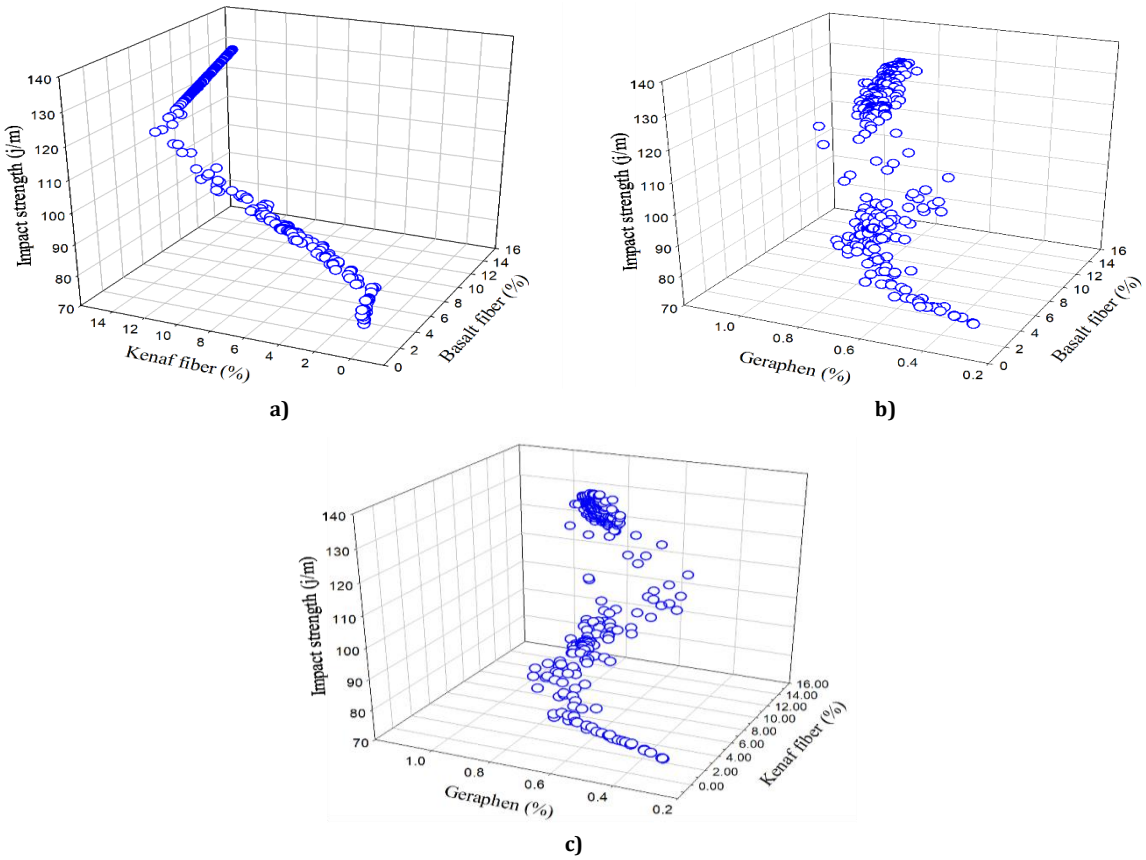

Fig. 10. Design variables distribution a) basalt fibers and kenaf fibers; b) basalt fibers and nanographene; c) kenaf fibers and nanographene in the best condition to boost the impact strength

The merits akin to the kenaf fibers, basalt, and graphene nanoparticles percentage as well as the optimum merits of preferable responses and also the position of these points in the scope of alterations employing the efficacy function technique are illustrated in Fig. 11 which is the state of the highest flexural strength along with the composite specimen lowest weight, and in Fig. 12 which is the maximum impact strength along with the composite specimen minimum weight. In addition, these points are one of the optimal solutions in the Pareto front shown in Fig. 8.

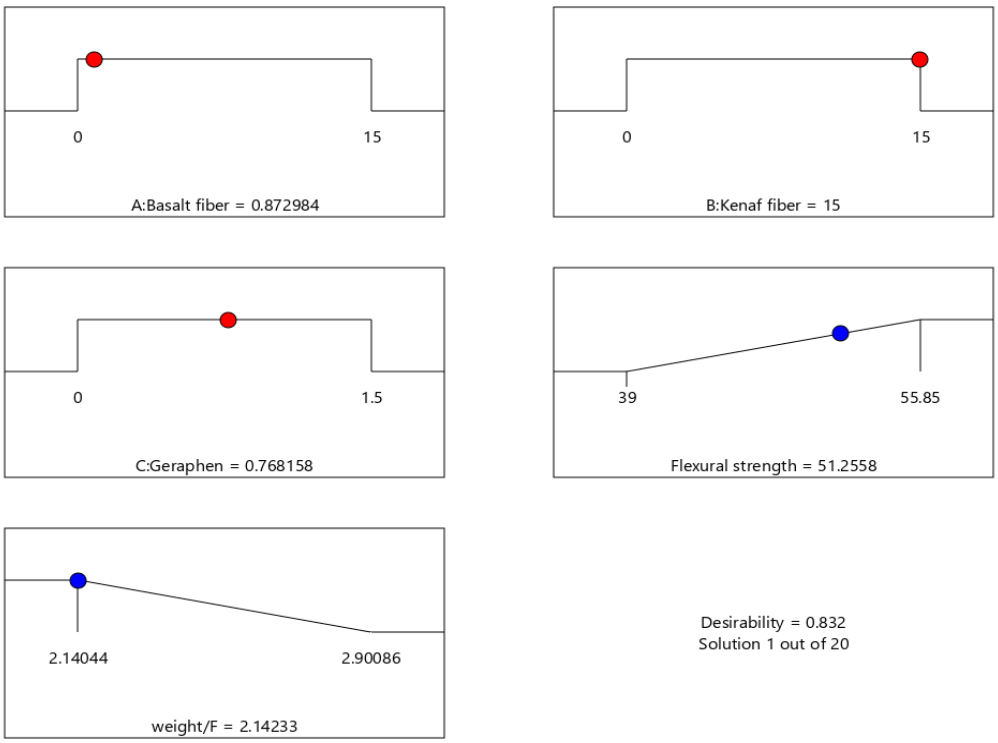

Fig. 11. Parameter and design responses optimum values in order to decrease the weight while increasing the flexural strength

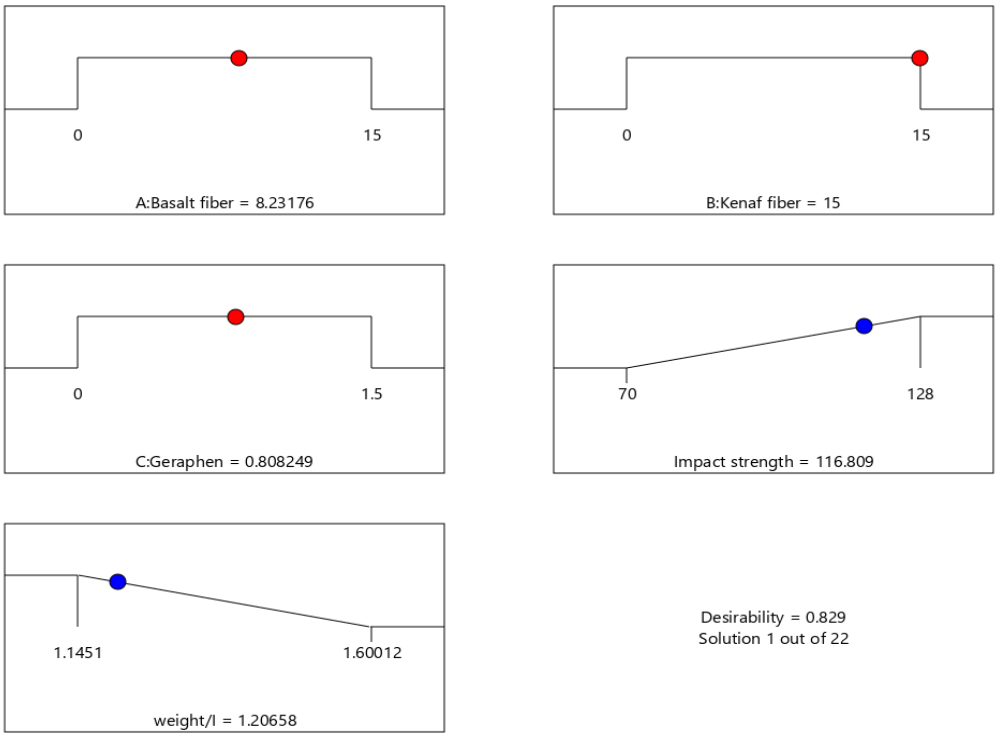

Fig. 12. Parameter and design responses optimum values in order to decrease the weight while increasing the impact strength

6. Conclusions

The impact of the basalt fibers weight percentage, graphene nanoparticles, and kenaf fibers on the flexural strength and impact behavior of basalt/PP/hemp/NG bio-composites was investigated in this study using BBD and RSM approaches. Moreover, the multi-objective optimization was done by the use of the MOPSO approach to boost the flexural and impact strength and reduce the introduced bio composite's weight. The general results are presented down below:

- Due to its high weight-to-strength ratio, kenaf fibers with a maximum value of 15 wt% are in the optimal specimens to increase the flexural and impact strength.
- FESEM images show that the fracture surface of the matrix is brittle during impact loading and the presence of the nanoparticles increases the adhesion of fibers to the polypropylene.
- The fracture of the substrate and the fibers are the main mechanisms of increasing the flexural strength and the fracture of the fibers along with the protrusion of the fibers out of the polypropylene matrix are also considered the key mechanism in boosting the impact strength.
- The optimal graphene nanoparticles' weight percentage which is presented in the introduced bio-composite for increasing the impact and flexural strength is 0.7681 and 0.8082%, respectively.
- Among the three independent parameters investigated, the content of kenaf fibers and basalt fibers possess the most contribution to the impact and the flexural strength, respectively.

7. Ethics Approval and Consent to Participate

The authors provided informed consent to enrolment in the study.

8. Consent for Publication

This is to state that I give my full permission for the publication and reproduction of the manuscript.

9. Availability of Data and Material

The data supporting the outcomes of this study are available based on the request from the corresponding author.

10. Competing Interests

For our article, entitled "Parametric Analysis and Multi-Objective Optimization of the Flexural and Impact Strength of Nanographene/Kenaf/Basalt Fiber-Reinforced Composites", which has been submitted to your journals for review, there is no conflict of interest.

Funding Statement

This research did not receive any specific grant from funding agencies in the public, commercial, or not-for-profit sectors.

Conflicts of Interest

The author declares that there is no conflict of interest regarding the publication of this article.

References

[1] Abdul Khalil, H.P.S., Nur Firdaus, M.Y., Anis, M., and Ridzuan, R., 2008. The Effect of Storage Time and Humidity on Mechanical and Physical Properties of Medium Density Fiberboard (MDF) from Oil Palm Empty Fruit Bunch and Rubberwood. Polymer-Plastics Technology and Engineering, 47 (10), 1046–1053, doi: 10.1080/03602550802355644.

[2] Azwa, Z.N. and Yousif, B.F., 2013. Thermal Degradation Study of Kenaf Fibre/Epoxy Composites Using Thermo Gravimetric Analysis. New South Wales, (January), 256–264.

[3] Gunawardene, O.H.P., Gunathilake, C., Amaraweera, S.M., Fernando, N.M.L., Wanninayaka, D.B., Manamperi, A., Kulatunga, A.K., Rajapaksha, S.M., Dassanayake, R.S., Fernando, C.A.N., and Manipura, A., 2021. Compatibilization of Starch/Synthetic Biodegradable Polymer Blends for Packaging Applications: A Review. Journal of Composites Science, 5 (11), 300, doi: 10.3390/jcs5110300.

[4] Karnani, R., Krishnan, M., and Narayan, R., 1997. Biofiber-reinforced polypropylene composites. Polymer Engineering & Science, 37 (2), 476–483, doi: 10.1002/pen.11691.

[5] Hamad, K., Kaseem, M., Ko, Y.G., and Deri, F., 2014. Biodegradable polymer blends and

composites: An overview. Polymer Science Series A, 56 (6), 812–829, doi: 10.1134/S0965545X14060054.

[6] Karnani, R., Krishnan, M., and Narayan, R., 1997. Biofiber-reinforced polypropylene composites. Polymer Engineering & Science, 37 (2), 476–483, doi: 10.1002/pen.11691.

[7] AZIZ, S., ANSELL, M., CLARKE, S., and PANTENY, S., 2005. Modified polyester resins for natural fibre composites. Composites Science and Technology, 65 (3–4), 525–535, doi: 10.1016/j.compscitech.2004.08.005.

[8] Rouison, D., Sain, M., and Couturier, M., 2004. Resin transfer molding of natural fiber reinforced composites: cure simulation. Composites Science and Technology, 64 (5), 629–644, doi: 10.1016/j.compscitech.2003.06.001.

[9] Taghipoor, H., Fereidoon, A., Ghasemi-Ghalebahman, A., and Mirzaei, J., 2023. Experimental assessment of mechanical behavior of basalt/graphene/PP-g-MA-reinforced polymer nanocomposites by response surface methodology. Polymer Bulletin, 80 (7), 7663–7685, doi: 10.1007/s00289-022-04420-x.

[10] Niyaraki, M.N., Mirzaei, J., and Taghipoor, H., 2023. Evaluation of the effect of nanomaterials and fibers on the mechanical behavior of polymer-based nanocomposites using Box–Behnken response surface methodology. Polymer Bulletin, 80 (9), 9507–9529, doi: 10.1007/s00289-022-04517-3.

[11] Albooyeh, A., Soleymani, P., and Taghipoor, H., 2022. Evaluation of the mechanical properties of hydroxyapatite-silica aerogel/epoxy nanocomposites: Optimizing by response surface approach. Journal of the Mechanical Behavior of Biomedical Materials, 136, 105513, doi: 10.1016/j.jmbbm.2022.105513.

[12] Jeyanthi, S. and Janci Rani, J., 2012. Improving mechanical properties by KENAF natural long fiber reinforced composite for automotive structures. Journal of Applied Science and Engineering, 15 (3), 275–280, doi:https://doi.org/10.6180/JASE.2012.15.3.08.

[13] Singh, J.I.P., Singh, S., and Dhawan, V., 2020. Influence of fiber volume fraction and curing temperature on mechanical properties of jute/PLA green composites. Polymers and Polymer Composites, 28 (4), 273–284, doi: 10.1177/0967391119872875.

[14] YU, T., LI, Y., and REN, J., 2009. Preparation and properties of short natural fiber reinforced poly (lactic acid) composites. Transactions of Nonferrous Metals Society of China, 19, s651–s655, doi: 10.1016/S1003-6326(10)60126-4.

[15] Lopresto, V., Leone, C., and De Iorio, I., 2011. Mechanical characterisation of basalt fibre reinforced plastic. Composites Part B: Engineering, 42 (4), 717–723, doi: 10.1016/j.compositesb.2011.01.030.

[16] Wu, G., Wang, X., Wu, Z., Dong, Z., and Zhang, G., 2015. Durability of basalt fibers and composites in corrosive environments. Journal of Composite Materials, 49 (7), 873–887, doi: 10.1177/0021998314526628.

[17] Wu, Z., Wang, X., Iwashita, K., Sasaki, T., and Hamaguchi, Y., 2010. Tensile fatigue behaviour of FRP and hybrid FRP sheets. Composites Part B: Engineering, 41 (5), 396–402, doi: 10.1016/j.compositesb.2010.02.001.

[18] Banibayat, P. and Patnaik, A., 2014. Variability of mechanical properties of basalt fiber reinforced polymer bars manufactured by wet-layup method. Materials & Design (1980-2015), 56, 898–906, doi: 10.1016/j.matdes.2013.11.081.

[19] High, C., Seliem, H.M., El-Safty, A., and Rizkalla, S.H., 2015. Use of basalt fibers for concrete structures. Construction and Building Materials, 96, 37–46, doi: 10.1016/j.conbuildmat.2015.07.138.

[20] Pham, T.M. and Hao, H., 2016. Review of Concrete Structures Strengthened with FRP Against Impact Loading. Structures, 7, 59–70, doi: 10.1016/j.istruc.2016.05.003.

[21] Furtos, G., Silaghi-Dumitrescu, L., Moldovan, M., Baldea, B., Trusca, R., and Prejmerean, C., 2012. Influence of filler/reinforcing agent and post-curing on the flexural properties of woven and unidirectional glass fiber-reinforced composites. Journal of Materials Science, 47 (7), 3305–3314, doi: 10.1007/s10853-011-6169-1.

[22] Furtos, G., Tomoaia-Cotisel, M., Baldea, B., and Prejmerean, C., 2013. Development and characterization of new AR glass fiber-reinforced cements with potential medical applications. Journal of Applied Polymer Science, 128 (2), 1266–1273, doi: 10.1002/app.38508.

[23] Ralph, C., Lemoine, P., Archer, E., and McIlhagger, A., 2019. Mechanical properties of short basalt fibre reinforced polypropylene and the effect of fibre sizing on adhesion. Composites Part B: Engineering, 176, 107260, doi: 10.1016/j.compositesb.2019.107260.

[24] Prodan, D., Moldovan, M., Furtos, G., Saroşi, C., Filip, M., Perhaiţa, I., Carpa, R., Popa, M., Cuc, S., Varvara, S., and Popa, D., 2021. Synthesis and Characterization of Some Graphene Oxide Powders Used as Additives in Hydraulic Mortars. Applied Sciences, 11 (23), 11330, doi: 10.3390/app112311330.

[25] Singh, K., Ohlan, A., and Dhaw, S.K., 2012. Polymer-Graphene Nanocomposites: Preparation, Characterization, Properties, and Applications. In: V. Mittal, ed. Nanocomposites - New Trends and Developments. Cambridge: InTech.

[26] Song, P., Cao, Z., Cai, Y., Zhao, L., Fang, Z., & Fu, S., 2011. Fabrication of exfoliated graphene-based polypropylene nanocomposites with enhanced mechanical and thermal properties. Polymer, 52 (18), 4001–4010.

[27] Yuan, B., Bao, C., Song, L., Hong, N., Liew, K.M., and Hu, Y., 2014. Preparation of functionalized graphene oxide/polypropylene nanocomposite with significantly improved thermal stability and studies on the crystallization behavior and mechanical properties. Chemical Engineering Journal, 237, 411–420, doi: 10.1016/j.cej.2013.10.030.

[28] basaltex, Basalt fiber composite fabric 9-17, [Online]. Available: https://www.nauticexpo.com/prod/cbg-composites-gmbh/product-198399-564726.html.

[29] American Society for Testing & Mater, 2002. Standard Test Methods for Flexural Properties of Unreinforced and Reinforced Plastics and Electrical Insulating Materials. D790. ASTM Stand., vol. i, pp. 1–12, doi: 10.1520/D0790-17.2.

[30] American Society for Testing & Mater, 1987. Standard Test Methods for Izod Pendulum Impact Resistance of Plastics. D256. ASTM Stand., vol. 10, no. Reapproved 2018, pp. 1–20, doi: 10.1520/D0256-10R18.N.

[31] Yaghoobi, H. and Fereidoon, A., 2018. An experimental investigation and optimization on the impact strength of kenaf fiber biocomposite: application of response surface methodology. Polymer Bulletin, 75 (8), 3283–3309, doi: 10.1007/s00289-017-2212-y.

[32] Yaghoobi, H. and Fereidoon, A., 2019. Thermal analysis, statistical predicting, and optimization of the flexural properties of natural fiber biocomposites using Box–Behnken experimental design. Journal of Natural Fibers, 16 (7), 987–1005, doi: 10.1080/15440478.2018.1447416.

[33] Shokrieh, M. M., & Ahmadi Joneidi, V., 2014. Manufacturing and experimental characterization of graphene/ polypropylene nanocomposites. Modares Mechanical Engineering, 13 (11), 55–63.

[34] Ary Subagia, I.D.G. and Kim, Y., 2013. A study on flexural properties of carbon-basalt/epoxy hybrid composites. Journal of Mechanical Science and Technology, 27 (4), 987–992, doi: 10.1007/s12206-013-0209-5.

[35] Tang, L.-C., Wan, Y.-J., Yan, D., Pei, Y.-B., Zhao, L., Li, Y.-B., Wu, L.-B., Jiang, J.-X., and Lai, G.-Q., 2013. The effect of graphene dispersion on the mechanical properties of

graphene/epoxy composites. Carbon, 60, 16–27, doi: 10.1016/j.carbon.2013.03.050.

[36] Sun, G., Tong, S., Chen, D., Gong, Z., and Li, Q., 2018. Mechanical properties of hybrid composites reinforced by carbon and basalt fibers. International Journal of Mechanical Sciences, 148, 636–651, doi: 10.1016/j.ijmecsci.2018.08.007.

[37] Deák, T. and Czigány, T., 2009. Chemical Composition and Mechanical Properties of Basalt and Glass Fibers: A Comparison. Textile Research Journal, 79 (7), 645–651, doi: 10.1177/0040517508095597.

[38] Ghasemi, F.A., Niyaraki, M.N., Ghasemi, I., and Daneshpayeh, S., 2021. Predicting the tensile strength and elongation at break of PP/graphene/glass fiber/EPDM nanocomposites using response surface methodology. Mechanics of Advanced Materials and Structures, 28 (10), 981–989, doi: 10.1080/15376494.2019.1614702.

[39] Eberhart, R. and Kennedy, J., 1995. A new optimizer using particle swarm theory. In: MHS'95. Proceedings of the Sixth International Symposium on Micro Machine and Human Science. IEEE, 39–43, doi: 10.1109/MHS.1995.494215.